Clinical Neurophysiology 147 (2023) 99–107

Contents lists available at ScienceDirect

Clinical Neurophysiology

journal homepage: www.elsevier.com/locate/clinph

Vagus nerve stimulation-induced laryngeal motor evoked potentials for response prediction and intensity titration in drug-resistant epilepsy

Alexandre Berger [a,b,c,*], Evelina Carapancea [a], Simone Vespa [a], Venethia Danthine [a], Pascal Doguet [b], Jean Delbeke [a,d], Antoine Nonclercq [a,e], Riëm El Tahry [a,f,g]

[a] Institute of Neuroscience (IoNS), Department of Clinical Neuroscience, Université Catholique de Louvain, Brussels, Belgium
[b] Synergia Medical SA, Mont-Saint-Guibert, Belgium
[c] Sleep and Chronobiology Lab, GIGA-Institute, CRC-In Vivo Imaging Unit, University of Liège, Liège, Belgium
[d] Institute of Neuroscience, LCEN3, Department of Neurology, Ghent University, Ghent, Belgium
[e] Bio, Electro and Mechanical Systems Department (BEAMS), Ecole Polytechnique de Bruxelles, Brussels, Belgium
[f] Center for Refractory Epilepsy, Department of Neurology, Cliniques Universitaires Saint-Luc, Brussels, Belgium
[g] Walloon Excellence in Life Sciences and Biotechnology (WELBIO) Department, WEL Research Institute, Avenue Pasteur 6, 1300 Wavre, Belgium

ARTICLE INFO

Article history:
Accepted 19 January 2023
Available online

Keywords:
Vagus nerve stimulation
Epilepsy
Larynx
Biomarker
Motor-evoked potentials
SVM

HIGHLIGHTS

- A support vector machine model based on laryngeal motor evoked potential features discriminated responders and non-responders with an accuracy of 80%.
- Responders received vagus nerve stimulation at an intensity between 1-fold and 2-fold the recruitment saturation of laryngeal motor evoked potentials, which may correspond to an optimal target.
- Laryngeal motor evoked potentials could be proposed as a guidance to scale vagus nerve stimulation intensity based on a physiological indicator of fiber engagement.

ABSTRACT

Objective: The objective of the study was to record Laryngeal Motor Evoked Potentials (LMEPs) in Vagus Nerve Stimulation (VNS)-implanted patients suffering from Drug-Resistant Epilepsy (DRE). Based on these recordings, LMEPs characteristics were evaluated and compared between responders (R) and non-responders (NR). Finally, possible under- or over-stimulation was assessed based on a physiological indicator of fiber engagement.
Methods: Mean dose–response curves were compared between R and NR. A Support Vector Machine (SVM) model was built based on both LMEP and dose–response curves features, to discriminate R from NR. For the exploration of possible under- or over-stimulation, a ratio between the clinically applied stimulation intensity and the intensity yielding to LMEP saturation was computed for each patient.
Results: A trend towards a greater excitability of the nerve was observed in R compared to NR. The SVM classifier discriminated R and NR with an accuracy of 80%. An ineffective attempt to overstimulate at current levels above what is usually necessary to obtain clinical benefits was suggested in NR.
Conclusions: The SVM model built emphasizes a possible link between vagus nerve recruitment characteristics and treatment effectiveness. Most of the clinically responding patients receive VNS at a stimulation intensity 1-fold and 2-fold the intensity inducing LMEP saturation.
Significance: LMEP saturation could be a practical help in guiding the titration of the stimulation parameters using a physiological indicator of fiber engagement.

* Corresponding author at: Institute of Neuroscience (IoNS), Department of Clinical Neuroscience, Université Catholique de Louvain, Brussels, Belgium.
E-mail address: alexandre.berger@uclouvain.be (A. Berger).

https://doi.org/10.1016/j.clinph.2023.01.009
1388-2457/

1. Introduction

Epilepsy is a serious neurologic condition associated with stigma, psychiatric comorbidity, and high economic costs. It is a common disorder with a reported prevalence of 6.38 per 1000 persons (Fiest, et al. 2017). One-third of patients are not rendered seizure-free with at least two antiepileptic drugs administered at correct dosages (Kwan, et al. 2010). In such cases, epilepsy is considered to be "refractory." Patients with a Drug-Resistant Epilepsy (DRE) need to be referred to a specialized epilepsy center for presurgical evaluation or alternative treatments. While brain resective surgery can be curative in carefully selected candidates, many patients cannot benefit from surgery because of multifocal seizure onset zones, generalized epilepsy, or when the seizure onset zone lies close to the eloquent cortex. In these patients, adjunctive treatments can be offered in an attempt to reduce seizure frequency and/or severity. Among the different approaches, Vagus Nerve Stimulation (VNS) is the least invasive and most widely used option. In most studies, the response rate to VNS varies between 45 and 66 % (Toffa, et al. 2020). In a study conducted on 362 implanted patients, the efficacy of VNS was proven to increase over time, with reported responder rates of 38.9 % and 58.8 % after 3 and 36 months of therapy, respectively (Kawai, et al. 2017). However, the mechanisms of action of VNS are not completely elucidated yet, and the biological requisites for responding to VNS are still a subject of research. In a clinical setting, there is a need for a cost-effective method to titrate stimulation of the vagus nerve in implanted patients. A titration biomarker based on individual physiological parameters is expected to be more pertinent than the actual empirical titration based on the subjective tolerance of the patients.

Stimulation of the vagus nerve co-activates the laryngeal motor fibers that branch off the vagus nerve at the level of the aortic arch and form the recurrent nerve. These low threshold motor fibers innervate the laryngeal muscles (except the cricothyroid) and part of the pharynx (Krahl, 2012). Therefore, VNS triggers recordable Laryngeal Motor Evoked Potentials (LMEPs) by activating low threshold A-fibers (El Tahry, et al. 2011). Indeed, studies that estimated the conduction velocity of the fibers responsible for the LMEP found values consistent with the known physiological properties of motor fibers (±45 m/s) (Vespa, et al. 2019, Bouckaert, et al. 2022). However, the therapeutic effects of VNS seem to be mediated by different myelinated afferent fibers characterized by a higher threshold (Aβ-, Aδ-, and B-fibers) (Evans, et al. 2004). It is worth mentioning that previous animal studies that reported antiseizure effects of VNS used current intensities below the threshold of B-fibers (Krahl, et al. 1998, Rijkers, et al. 2010, Raedt, et al. 2011), emphasizing the likely role of Aβ- and/or Aδ-fibers in the antiseizure effects of VNS. Since properties of fibers such as the conduction velocity, the diameter, or the threshold for electrical activation are intrinsically related (Woodbury and Woodbury 1990, Boyd and Kalu 1979), it could be hypothesized that a constant ratio exists between stimulation parameters obtained from LMEPS (i.e., current intensity and pulse width – the charge) and vagus nerve fibers carrying the antiepileptic effects.

Previous studies successfully recorded LMEPs invasively in VNS-implanted rats (El Tahry, et al. 2011, Grimonprez, et al. 2015) and humans through intra-operative vocal cord recording or needle EMG during laryngoscopy (Ardesch, et al. 2010, Kamani, et al. 2015). The invasive measurement of LMEPs is a laborious procedure that could be performed only during the implantation of a VNS device. It has been shown that surface electrodes in a horizontal neck derivation allow non-invasive LMEP recording in humans (Vespa, et al. 2019). Based on this technique, studies successfully recorded LMEPs in chronically and acutely implanted patients with DRE and hypothesized that LMEPs could be used as a biomarker of a genuine vagal A-fiber activation (Vespa, et al. 2019, Bouckaert, et al. 2022).

The goal of the present study was to record LMEPs in VNS-implanted patients using a non-invasive, easy-to-record, and cost-effective technique to assess the neurophysiological properties of VNS-activated low threshold motor fibers and correlate them with the clinically programmed parameters in patients. Single compound motor action potential parameters and recruitment-related characteristics were obtained from LMEP recordings. Moreover, the clinically applied stimulation currents were compared to the intensity leading to saturation of the LMEP motor fibers. Finally, a Support Vector Machine (SVM) model was built to determine how accurately recruitment-related LMEPs characteristics could discriminate Non-Responders (NR) from Responders (R).

2. Material and methods

2.1. Data acquisition

2.1.1. Patients

Patients included in the present study were recruited from the VNS database of the Center for Refractory Epilepsy of Saint-Luc University Hospital, Brussels, Belgium. Data included in the study are from patients who met the following criteria: (i) DRE diagnosis; (ii) treated with VNS (DemiPulse Model 103 or DemiPulse Duo Model 104, AspireHC Model 105 or AspireSR Model 106; LivaNova, Inc., London, United Kingdom) for at least three months and (iii) aged between 18 and 75 years. Exclusion criteria consisted of severe side effects due to VNS therapy, such as dyspnea or severe pain in the neck or the ear region. The clinical response evaluation was determined at the last follow-up visit. All patients signed the informed consent prior to any investigation. The Ethics Committee of Saint-Luc Hospital approved the study procedures (Reference No. 2018/07NOV/416).

2.1.2. Recording method

Patients numbered 1–11 were included in a formerly published study by Vespa et al. (Vespa, et al. 2019), in which an EEG/EP digital acquisition system (Matrix 1005, Micromed, Mogliano Veneto, Italy) was used for recording LMEPs. For the other patients (numbered 12–45), LMEPs were recorded using the Biosemi (Amsterdam, Netherlands) EEG/EP acquisition system. The sampling rate was set at 4096 Hz. Signals were high pass filtered at 0.5 Hz. LMEPs were recorded with two recording surface electrodes in a horizontal bipolar derivation (LMEP+/LMEP-), as described in (Vespa, et al. 2019).

2.1.3. Stimulation protocol

The impedance of the VNS lead was checked before and after the session. Patients were instructed to minimize neck movements and to abstain from speaking except to report discomfort or pain due to the stimulation. The therapeutic parameters, including the stimulation current (I_{stim} expressed in mA), frequency (Hz), pulse width (μs), and duty cycle (%), were checked at the beginning of the session. For the initial phase, I_{stim} was set to 0 mA (VNS OFF), while the frequency remained unchanged. The pulse width used in patients numbered 1–11 previously included in (Vespa, et al. 2019) (and also included in the present study) was set to 250 μs. For the remaining patients (numbered 12–45), the pulse width was kept at the clinically programmed pulse width (250 or 500 μsec). The external magnet was programmed to stimulate at gradually increasing intensities, with 0.25 mA increments up to 0.125

Table 1
Demographic and clinical characteristics of the study population (n = 42, 20 Non-Responders - NR, 22 Responders - R). M: Male, F: Female. * Duty cycles are determined based on previously reported definitions (Kayyali, et al. 2020, DeGiorgio, et al. 2005, Heck, Helmers and DeGiorgio 2002, Yamamoto 2015).

Variables	NR (n = 20)	R (n = 22)	p-value
Sex	9 M – 11F	9 M – 13F	0.79
Age	40.8 (±15.59)	42.04 (±16.58)	0.80
Epilepsy onset age	18.95 (±13.54)	13 (±9.47)	0.10
Duration VNS therapy (months)	66.7 (±47.74)	82 (±70.41)	0.41
Mean VNS output current (mA)	1.5 (±0.40)	1.41 (±0.34)	0.38
Mean VNS frequency (Hz)	24.75 (±4.44)	24.77 (±4.75)	0.98
Mean VNS pulse width (μs)	300 (±102.6)	295.45 (±98.7)	0.88
Rapid duty cycle *	2 (14 s ON/66 s OFF – 23 %) (30 s ON/66 s OFF – 35 %)	1 (14 s ON/66 s OFF – 23 %)	
Epilepsy type:			
Focal epilepsy	18	16	
Generalized epilepsy	2	6	

or 0.25 mA higher than the clinically applied stimulation current (Fig. 1A), depending on the tolerance of the patient.

Using the external magnet, six trains of 14 s were delivered for each stimulation intensity level, three in the ascending and three in the decremental phase (Fig. 1A). Ramp-up and ramp-down phases occurred at the initiation and at the end of each stimulation, and lasted 2 s each. Therefore, each stimulation train lasted 18 s in total (Fig. 1B). A period of 40 s of VNS OFF was taken between each stimulation train. At the end of the experiment, I_{stim} was reset to the clinically applied output current, and the lead impedance was checked to be under 5 kΩ.

2.2. Data analysis

2.2.1. Demographic and clinical features

Demographic and clinical features of patients included in the study, including sex, age, type of epilepsy, epilepsy onset age, duration of VNS therapy, VNS current, VNS frequency, VNS pulse width, and VNS duty cycle (time ON/time OFF) are reported in Table 1. These features were statistically compared between R and NR, using Mann-Whitney U-tests.

2.2.2. LMEP features

After the recording, signals were analyzed using MATLAB 2018a software (MathWorks, Natick, MA, United States). To remove data acquired during the ramp-up and ramp-down phases, the 2 s at the beginning and at the end of each stimulation block were discarded. Fifty consecutive stimulations were time-marked for each VNS train administered, starting 1 s after the ramp-up period to ensure stabilization, by using an automatic VNS stimulation artifact identification algorithm. Thereafter, the selected 50 trains were segmented into epochs according to the method described in (Vespa, et al. 2019). A visual analysis was conducted to ensure that possible movements did not impact the recordings. The peak-to-peak

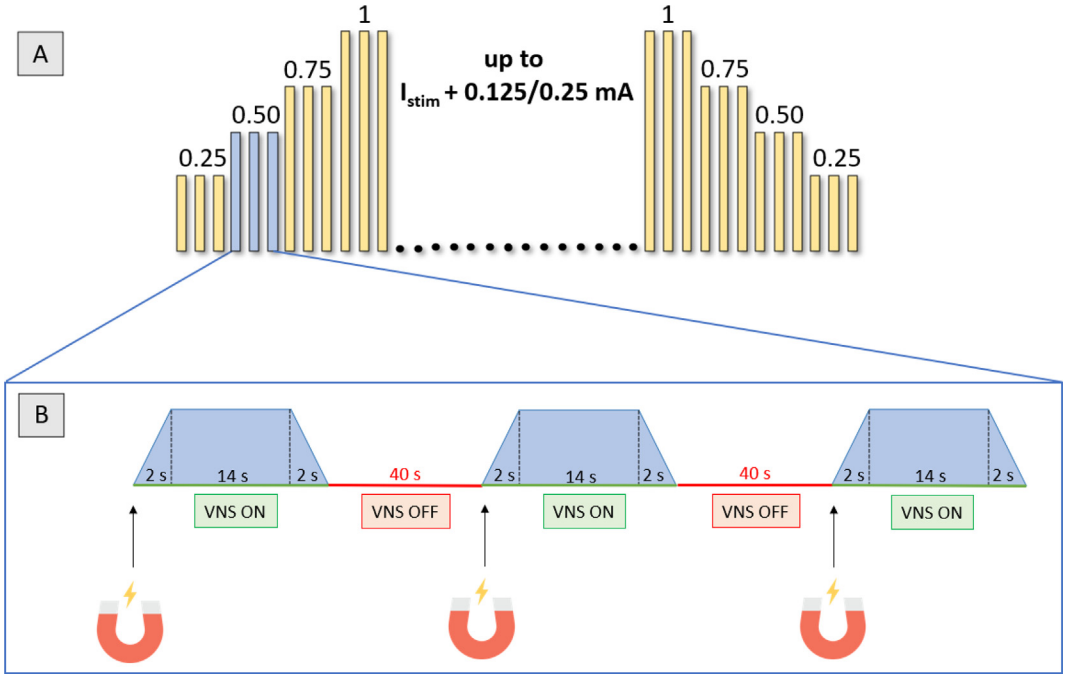

Fig. 1. (A) Timeline of the stimulation protocol. (B) Magnet-induced stimulations and duration of each stimulation block. I_{stim}: clinically applied stimulation current, mA: milliamperes, s: seconds, VNS: Vagus Nerve Stimulation.

(P2P) amplitude value was computed for each single LMEP waveform as the difference between the largest positive and negative deflections occurring after the stimulation artifact. The following P2P values were averaged, obtaining a P2P mean value and standard deviation (SD) for each stimulation epoch. Finally, P2P amplitudes were averaged across the epochs corresponding to the same stimulation current values (6 epochs in total), resulting in a mean P2P amplitude and SD for each current intensity and for each subject.

The LMEP latency, extracted after computation of the first derivative of the signal (when clinical stimulation parameters are used, such as I_{stim} and the pulse width), was defined as the time between the initial peak of the stimulation artifact and the initial deflection of the motor response (Vespa, et al. 2019). The measured LMEP latency was normalized by patient's height to take differences in nerve length into account. The height-corrected latency (L_c) of a patient was computed as follows: *(latency/height of the patient) * (average height of the patients in the investigated cohort)*. The value of the maximal LMEP amplitude, corresponding to the plateau of the recruitment curve (Y_{sat}), was measured for all the patients included in the study. Recruitment-unrelated LMEP characteristics (L_c and Y_{sat}) were extracted in all patients with recordable LMEPs and were compared between R and NR using Mann-Whitney U-tests.

2.2.3. LMEP recruitment: dose–response curves

A Boltzmann sigmoid function was used to fit LMEPs amplitudes as a function of the stimulation charge (current × pulse width) (Devanne, Lavoie and Capaday 1997). Since the charge rather than the stimulation current alone is known to better reflect the actual activation of the nerve fibers, the charge instead of the current amplitude alone was used for the fitting. The recruitment curves (or dose–response curves) were obtained for each patient using the MATLAB 2018a Curve Fitting Toolbox. The corresponding LMEP amplitude, as a function of the stimulation charge (C_S), was modeled as:

$$LMEP\ amplitude = \frac{Y_{sat}}{\left[1 + e^{\frac{(C_{50} - C_S)}{k}}\right]} \quad (1)$$

The Boltzmann fit was considered to be good whenever the curve showed a $R_2 > 0.95$ and ≥ 2 points on the ascending part of the curve (Bouckaert, et al. 2022, Vespa, et al. 2019). Only patients with good fit of the dose–response curve, and for whom a pulse width of 250 μs was used, were candidates to extract the following features which were subsequently compared between R and NR:

- C_{50} – Charge for an output current value at which the LMEP amplitude reaches half its maximal amplitude [nC].
- C_{98} – Charge for an output current value leading to 98 % recruitment of the fibers [nC].
- k – Recruitment slope value corresponding to the fiber excitability homogeneity.
- C_5 – The charge leading to 5 % recruitment of the fibers is taken as a theoretical threshold for LMEP induction [nC].

2.2.4. Optimal range of therapeutic current based on fibers saturation

Regardless of the goodness of the Boltzmann fit based on the criteria mentioned above, the curve enabled us to obtain confidence intervals (CI) for the levels of Y_{sat} (since a saturation is observed, independently of the slope of the curve). Hence, by using such intervals, the lowest output current value administered that was falling within the range of the CI of Y_{sat} was determined and used to estimate the intensity needed for LMEP saturation (I_{sat}) in *all* patients. The ratio between the routinely used output current and the previously described estimate of LMEP saturation, defined as I_{stim}/I_{sat}, was compared between R and NR for all the patients included in the study. In that regard, the mean and standard deviation of the I_{stim}/I_{sat} ratio was computed for R and NR, and the Probability Density Function (PDF) of this ratio was estimated for R and NR using a kernel density non-parametric method ("ksdensity" MATLAB 2018a built-in function) (Hill 1985). Eventually, the probability (the area under the PDF curve) that the I_{stim}/I_{sat} ratio lies in a given range of integer values (0–1, 1–2, 2–3, 3–4, and 4–5) was computed for R and NR using trapezoidal numerical integration ("trapz" MATLAB 2018a built-in function).

2.2.5. SVM and multi-feature classification

Only subjects showing a good fit of the Boltzmann curve (and for whom a pulse width of 250 μs was used during the stimulation protocol) were included in the discovery cohort used to train the SVM classifier. The SVM model was built using the Scikit-learn machine learning library (French Institute for Research in Computer Science and Automation, Rocquencourt, France) implemented in Python (Pedregosa, et al. 2011).

Feature selection was conducted using a recursive feature elimination technique. A wrapper feature selection method that uses an internal filter-based feature selection was used to rank the features by importance. Therefore, (i) six features of interest (Y_{sat}, C_{50}, C_{98}, k, C_5, L_c) were ranked based on their p-value computed with Mann-Whitney U-tests between the two groups (R and NR), then (ii) a model was fitted using all the features of interest and (iii) features were recursively discarded based on their p-value, before refitting the model. When fitting an SVM model, it is common to use kernel functions to implicitly map the data into a higher-dimensional space. This technique is used to make non-linear data linearly separable in a higher dimensional space, where a linear classifier can be used to separate the data. Different kernel functions were used (linear kernel, polynomial kernel, Radial Basis Functions – RBF, and sigmoid kernel) and compared in terms of accuracy to select the most suited SVM classifier.

The classifier accuracy was evaluated using the Leave-One-Out (LOO) cross-validation technique. Grid search (a technique used to tune and identify the optimal hyperparameters in a model) was used to select the regularization parameter (C) and the gamma-kernel coefficient (γ - only applicable for the polynomial kernel, RBF and sigmoid kernel) for fitting the soft-margin SVM model. The C parameter ensures a tradeoff between misclassifications and maximization of the margin hyperplane for a better generalization of the model to unknown data. The γ parameter controls the distance of influence of a single training point and therefore influences the curvature of the decision boundary. Grid search was conducted by searching over values of $C = [2^{-5}, \ldots, 2^{2}]$. The optimal model (i.e., the best-performing kernel function, the best subset of features, and most suited hyperparameters) was selected based on the classification accuracy of the different models tested. Thereafter, the confusion matrix reporting the true positive (TP), true negative (TN), false positive (FP), and false negative (FN) predictions were computed. The sensitivity (or true positive rate) defined as TP/(TP + FN) and the specificity (or true negative rate), i.e., TN/(TN + FP), finally led to an estimation of the Area Under the Curve (AUC) of the Receiver Operating Characteristic (ROC) curve of the best SVM classifier.

3. Results

3.1. LMEP recording and single-feature analysis

In total, 45 patients were eligible and recruited. The LMEPs could not be recorded in 3 patients. One of them (a NR) presented

a history of postsurgical laryngeal nerve lesion. However, no history of injured left laryngeal nerve, or vocal cord dysfunction was reported in the two other patients (one R and one NR). Therefore, 42 patients in whom LMEPs were successfully recorded were finally included in the study (22 R and 20 NR). The demographic and clinical characteristics of the included patients are reported in Table 1.

LMEPs features were extracted, as summarized in Table 2A. Although not significant (at the level $p < 0.05$), a slight increase in the latency was observed in the NR (7.70 ± 1.36 ms) compared to the R (7.61 ± 0.98 ms). Moreover, a trend towards a lower Y_{sat} was observed in NR (191.77 ± 88.9 μV) compared to R (209.85 ± 9 7.7 μV).

The Boltzmann curve was successfully fitted in 17/42 patients (9 R and 8 NR), including 15 patients for whom a pulse width of 250 μs was used. Recruitment-related LMEPs characteristics of these patients are summarized in Table 2B. The mean dose–response curve of patients showing a good fit of the Boltzmann curve was computed for R and NR, as shown in Fig. 2. Although not significant, a trend toward an earlier rising flank of the dose–response curve was observed in R compared to NR, as reflected by a lower C_5 in R (56.42 ± 38.94 nC) compared to NR (68.93 ± 50.1 nC). Moreover, a trend toward a lower C_{50} was observed in R (129.97 ± 31. 19 nC) compared to NR (154.83 ± 49.27 nC), without reaching a significance level at level $p < 0.05$.

3.2. Optimal range of therapeutic current based on fibers saturation

The PDF of the I_{stim}/I_{sat} ratio was estimated for each patient. The estimated PDF for R and NR are shown in Fig. 3. In the R group, the distribution of I_{stim}/I_{sat} is sharper than the distribution for NR, which spreads over a wider range of values instead. Moreover, probabilities of I_{stim}/I_{sat} to lie within different ranges of integer ratios were computed for R (Fig. 3B) and NR (Fig. 3C). According to the results, there is a probability of 68.5 % that patients predisposed to becoming R to VNS will have a clinical output current set to a value within a range of 1-fold and 2-fold the intensity that induce LMEP saturation. This probability drops to 38.27 % for the NR group.

Table 2
Comparison of Laryngeal-Motor Evoked Potentials (LMEPs) characteristics between responders (R) and non-responders (NR). (A) Recruitment-unrelated features extracted in all patients (42 patients, 20 NR, 22 R) with recordable LMEPs, and (B) Recruitment-related LMEP features in patients with a good fit of the Boltzmann curve and for whom a pulse width of 250 μs was used as part of the stimulation protocol (15 patients, 7 NR, 8 R). The mean (and standard deviations) values are reported in the table.

A. Recruitment-unrelated characteristics (42 subjects)	**NR (n = 20)**	**R (n = 22)**	**p-value**
L_c (ms)	7.70 (±1.36)	7.61 (±0.98)	0.81
Y_{sat} (μV)	191.77 (±88.9)	209.85 (±97.7)	0.53
B. Recruitment-related characteristics (15 subjects)	***NR (n = 7)***	***R (n = 8)***	***p-value***
k (slope)	29.17 (±8.91)	24.97 (±8.55)	0.34
C_{50} (nC)	154.83 (±49.27)	129.97 (±31.19)	0.34
C_{98} (nC)	268.37 (±66.58)	227.18 (±46.92)	0.34
C_5 (nC)	68.93 (±50.1)	56.42 (±38.94)	0.69

3.3. SVM and multi-feature classification

The ranking of the features extracted from the Boltzmann fit was: k ($p = 0.34$), C_{50} ($p = 0.34$), C_{98} ($p = 0.34$), Y_{sat} ($p = 0.46$), C_5 ($p = 0.69$) and L_c ($p = 1$). Since three features presented the same p-value, the recursive feature elimination was conducted until the three most discriminatory features were used for the classification. The best-performing model was using the sigmoid kernel function for mapping the data, and the top 4 features for the classification, including k, C_{50}, C_{98}, Y_{sat} (Fig. 4A). A summary of the performance of the different models (subsets of features with the corresponding best-performing hyperparameters) can be found in the Supplementary Material S1.

Grid search over the hyperparameters suggested a top-performing classification for values of $C = 4$ and $\gamma = 1$ (Fig. 4B). The corresponding sensitivity and specificity for the best-performing hyperparameters are also shown in Fig. 4B. The confusion matrix that summarizes the classification predictions and the ROC curve of the best-performing model are shown in Fig. 4C. Using this model, the classifier reached an accuracy of 80 %, a sensitivity of 75 %, and a specificity of 85.71 %. Finally, based on the ROC curve, the final SVM classifier reveals an AUC of 82.1 %. It is worth mentioning that a model using a sigmoid kernel and six features for the classification also reached a classification accuracy of 80 %, with a corresponding sensitivity of 87 % and a specificity of 71.41 %. Due to the lower specificity of the model compared to the previous one and the poor corresponding AUC (64.3 %), the final model used for the classification is the one using four features.

4. Discussion

In the current study, LMEPs were successfully recorded in 42/45 patients, showing a good reproducibility of the recording technique that was previously described in (Vespa, et al. 2019). The mean I_{stim}/I_{sat} ratio was larger in the NR group than in the R group, suggesting in the NR group an ineffective attempt to overstimulate at current levels above what is usually necessary to obtain clinical benefits. The peak-like PDF of the I_{stim}/I_{sat} ratio observed in R may suggest that given the stimulation level of motor fiber saturation, an optimal range of stimulation current with antiseizure effects could be estimated in these patients. When looking at the I_{stim}/I_{sat} ratio in NR, a rather dispersed distribution was observed, reflecting the heterogeneity of causes behind the non-response. Indeed, NR with a ratio lower than the optimal range of output currents related to saturation of low-threshold A-fibers, could correspond to more sensitive patients who do not tolerate VNS well and therefore are not stimulated at current intensities sufficient to observe antiseizure effects. Alternatively, if an adequate treatment remains inefficient despite intensities in the effective range, more central mechanisms must be considered. In this case, other parameters affecting the synaptic transmission, such as the pulse frequency or train length could be adapted (Loerwald, et al. 2018). A previous study which used a generalized linear mixed model to ascertain the relationship between key stimulation parameters and clinical outcome in 1178 patients, has demonstrated a population level optimal target output current and duty cycle at 1.61 mA and 17.1 % (Fahoum, et al. 2022). In addition to this target dose, an inverted-U relationship has been reported between VNS intensity and brain plasticity in specific areas. This principle was demonstrated in studies where VNS was paired with motor training in rats to improve recovery after neurological injury. Intracortical microstimulation was used to infer plasticity effects, based on the movement representations in the motor cortex (Morrison, Hulsey, et al. 2020, Morrison, Danaphongse and Abe, et al. 2021, Morrison, Danaphongse and Pruitt, et al. 2020). Other studies in

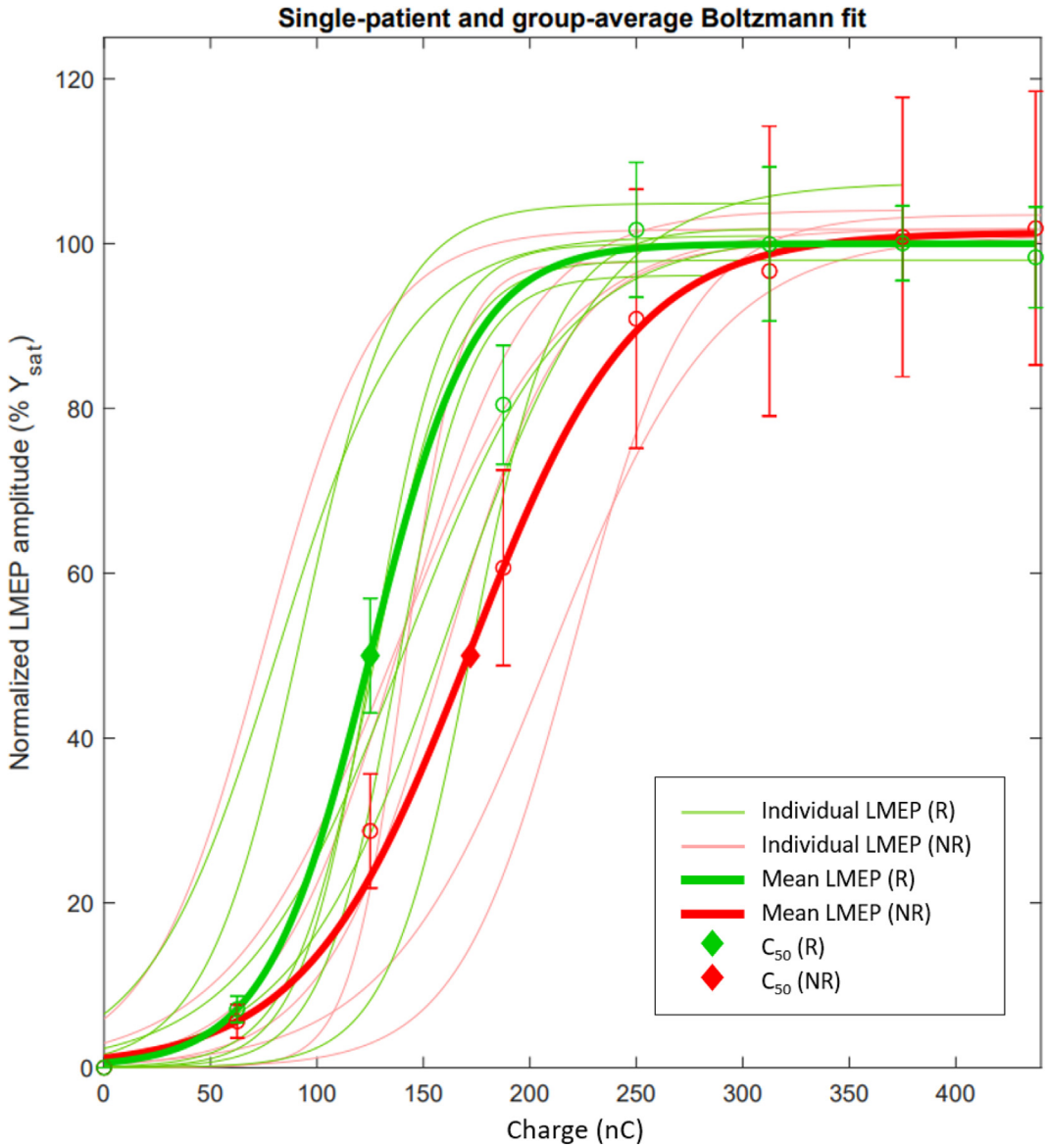

Fig. 2. Normalized (% Y_{sat} – the value of the maximal LMEP amplitude, corresponding to the plateau of the recruitment curve) single-patient dose–response curves and normalized fitted Laryngeal-Motor Evoked Potential (LMEP) values averaged across responders (R, green, n = 8) and non-responders (NR, red, n = 7). C_{50}: Charge for an output current value at which the LMEP amplitude reaches half its maximal amplitude [nC].

the field of stroke recovery and fear conditioning for Posttraumatic Stress Disorder (PTSD) also suggested an inverted-U relationship as assessed respectively with motor tasks and behavioral tests (Pruitt, et al. 2021, Souza, et al. 2021). In opposition to the sigmoid relationship found for the VNS-induced LMEPs, it could be hypothesized that the inverted-U relationship found at the central level may be due to the additional recruitment of a high-threshold inhibitory or desensitizing system.

We should acknowledge that no significant differences in single LMEP features were found between R and NR, which is concordant with results reported by Bouckaert et al (Bouckaert, et al. 2022). Nevertheless, individual dose–response curves reveal a trend toward greater excitability of the nerve fibers in R compared to NR. Indeed, a trend towards an earlier rising flank of the dose–response curve, a lower charge leading to half-saturation of the fibers, and a lower excitability threshold were observed in R compared to NR. A multi-feature analysis using SVM was conducted to evaluate whether features extracted from the dose–response curve could accurately discriminate NR from R. Using four features for the classification (i.e., the slope of the dose–response curve, the charge leading to 50 % saturation of the fibers, the charge leading to 98 % saturation of the fibers and the amplitude of the LMEP at the plateau phase of the recruitment curve), the SVM model reached a classification accuracy of 80 %, a sensitivity of 75 %, a specificity of 85.71 % and an AUC of the ROC curve of 82.1 %. Despite the difficulty of interpretability of our machine learning forecast in clinical terms, the model built in the present study emphasizes a possible link between vagus nerve recruitment characteristics and the treatment effectiveness.

It was previously suggested that a low stimulation current (ranging from 0.25 to 0.75 mA for a pulse width of 250 μs) was sufficient to record LMEPs (Bouckaert, et al. 2022). This observation was confirmed in the present study, where the mean theoretical threshold reflecting the charge needed for the recruitment (5 % saturation) of motor fibers was approximately 69 nC (corresponding to an output current of 0.27 mA for a pulse width of 250 μs) and 56 nC (corresponding to an output current of 0.22 mA for a pulse width of 250 μs) in NR and R, respectively. It is worth mentioning

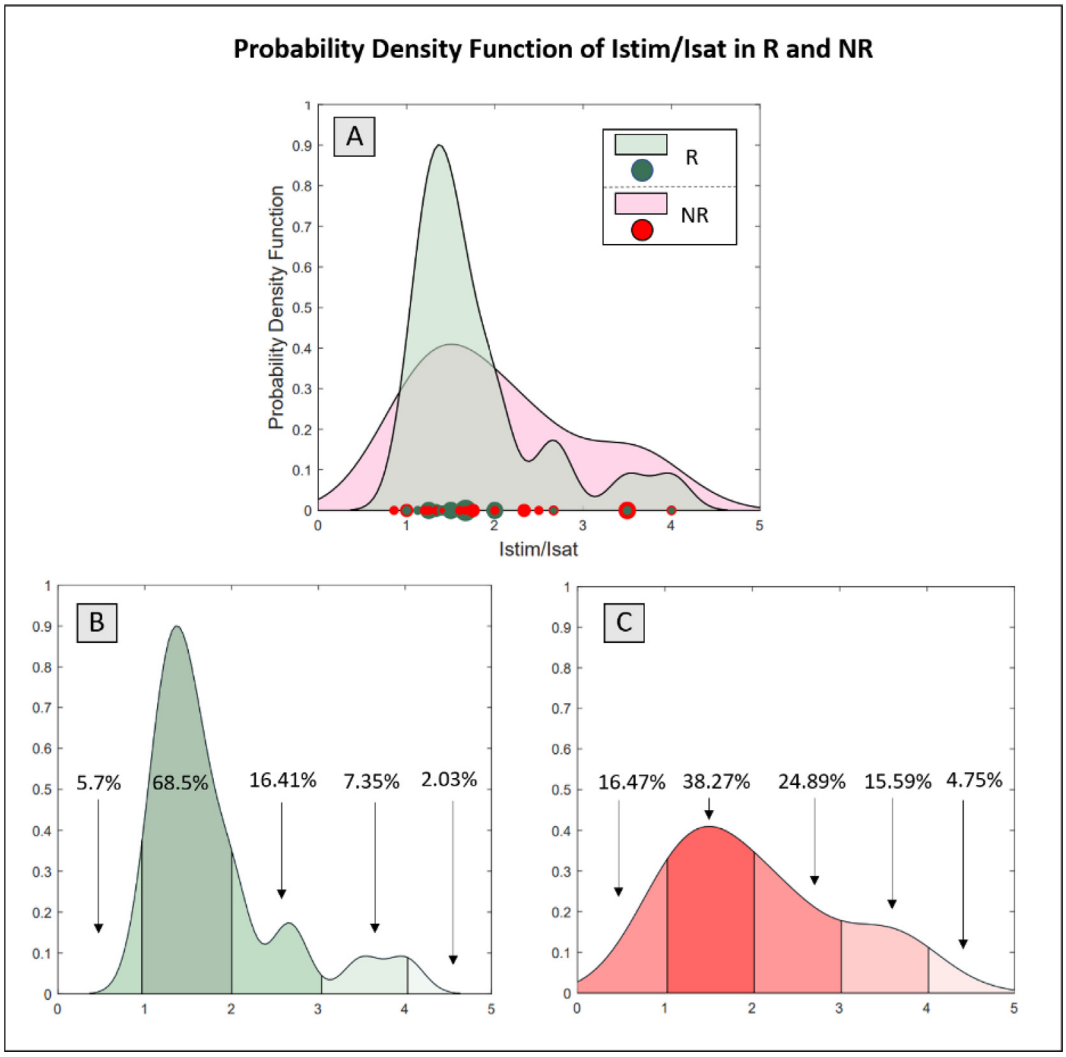

Fig. 3. Probability Density Function (PDF) of the ratio between the routinely used output current (I_{stim}) and the intensity needed for LMEP saturation (I_{sat}) estimated in responders (R, green, n = 22) and non-responders (NR, red, n = 20). (A) The ratios I_{stim}/I_{sat} of the patients are represented by circles, with the size being proportional to the number of patients with the same ratio. Probability that I_{stim}/I_{sat} lies within different ranges of integer ratios for (B) R and (C) NR.

that these values were recorded for VNS devices composed of a similar spiral electrode placed around the vagus nerve. The values could be different for another electrode design, such as a cuff electrode. In addition, a previous study showed that the threshold current for minimal response induction was stable over time (Bouckaert, et al. 2022). Therefore, LMEPs could give insight into the state of the nerve and the nerve-electrode contact early after the implantation of a VNS device. In R, a charge of approximately 130 nC was found on average to recruit half the motor fiber population. Since a pulse width of 250 μs was used in these patients, this charge corresponds to an output current of 0.51 mA. Therefore, almost all motor fibers are probably responding at approximately 1 mA. However, on average, our results suggest that full recruitment in NR requires approximately 155 nC, corresponding to 1.2 mA. Higher threshold in NR could be due to a partially damaged nerve (demyelination), anatomical differences such as the relative position of fibers within the nerve, the electrode contact position, or the local tissue gliosis (Bouckaert, et al. 2022). Although a broad spectrum of causes may underlie non-response, these results reinforce the idea that a reduced excitability of the nerve leading to an inadequate activation could be involved in (at least part) of NR included in the present study.

However, the current study presents several limitations. In 3/45 patients no LMEP recording was possible. The absence of LMEP recording may be explained by different physiological problems (e.g., an inefficient activation of vagal fibers due to postsurgical scarring or gliosis, axonal degeneration, or a concomitant pathology), or technical difficulties during the recording. One of the patients (a NR) in whom LMEPs were not recorded presented a history of left recurrent laryngeal nerve injury after a thoracic surgery unrelated to VNS therapy. For the two other patients (one R and one NR), no clinical history of injured left laryngeal nerve or vocal cord dysfunction was reported, but no laryngoscopy was performed. A second limitation is the fact that a successful fitting of the Boltzmann curve (at least two points on the rising flank of the curve) was achieved in 17/42 patients only. Newer versions of VNS devices should allow for smaller stimulation intensity increments and therefore more points on the rising flank for a better fitting of the dose–response curve. The cohort in the present study included patients chronically implanted for up to 10 years, which only held titration steps of 0.25 mA.

In future studies, an independent cohort of patients could be used as a validation cohort to further evaluate the reproducibility of the proposed SVM classifier on unknown data. Moreover, further

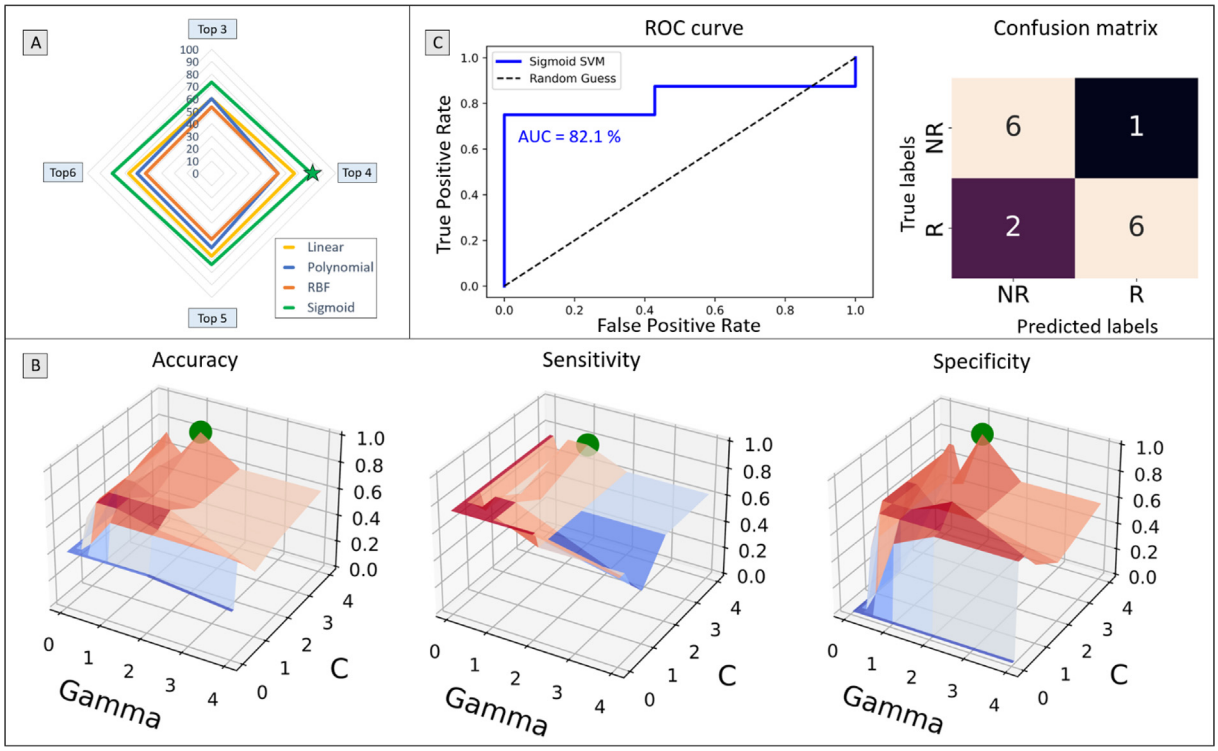

Fig. 4. Model selection: (A) Recursive Feature Elimination (RFE) for the top 3 features, top 4 features, top 5 features, and all 6 features with the corresponding maximum accuracy of classification for models when different kernels (linear kernel, polynomial kernel, Radial Basis Function - RBF and sigmoid kernel) are used. (B) For the model with the best accuracy (80 %, sigmoid kernel function), details of the grid search over the hyperparameters (C and γ) are shown. The green sphere represents the [C, γ] combination leading to the best accuracy. The corresponding sensitivity and specificity are also shown. (C) Receiver Operating Characteristic (ROC) curve of the final Support Vector Machine (SVM) classifier, with an Area Under the Curve (AUC) of 82.1 % and the confusion matrix of the final SVM classifier (top 4 features, sigmoid kernel, C = 4, γ = 1), showing 6 true positive predictions, 6 true negative predictions, 1 false positive prediction and 2 false negative predictions, resulting in a sensitivity of 75 %, and a specificity of 85.71 %.

investigations studying the relationship between the recruitment of low threshold motor fibers and the afferent central antiepileptic fibers of the vagus nerve, are necessary. Non-invasive techniques such as functional magnetic resonance imaging, electroencephalography, or pupillometry could be used to build a classification model combining efferent markers of effective nerve stimulation with afferent markers of central VNS effects involved in the antiseizure effects of the treatment. Building such a model could help to deepen our current knowledge about the (possibly co-acting) mechanisms responsible for non-response in approximately 1/3 of implanted patients and help to stratify these patients better.

5. Conclusion

Using a non-invasive, easy-to-record, reproducible, and cost-effective technique, LMEPs were recorded in VNS-implanted patients suffering from refractory epilepsy. Clinically applied stimulation levels in R and NR have been compared with the recorded motor response in the recurrent nerve branch. The results suggested that most of the clinically responding patients receive VNS at a stimulation intensity 1-fold and 2-fold the intensity inducing LMEP saturation. Our results clearly indicate that non-response can have several different causes, as reflected by the inhomogeneity in the non-responding group. When a stimulation below that "optimal" level is used in NR, one could suggest an ineffective stimulation of the vagus nerve where the stimulation intensity should be increased, given that no side effect prevents it. For NR with a stimulation level above the usually effective range might reflect a desperate attempt to obtain a response by increasing the intensity. Based on these results, we support the idea that scaling the stimulation intensity as a function of the LMEP saturation could be a practical help in guiding the titration of the stimulation parameters using a physiological indicator of fiber engagement. Indeed, measuring LMEPs could provide a stimulus strength reference in a single patient and indicate when increasing the intensity or pulse duration becomes useless. Therefore, knowing that the nerve is activated effectively can then be the rational basis on which the clinician can try to further improve an ineffective treatment by changing the pulse train duration or frequency: two stimulation parameters known to be involved in the central effects of VNS by acting on central synapses. In the future, LMEPs could be used in the clinical context to give early hints on the success of implantation, monitor the evolution of the recovery of the nerve, and perhaps improve the adequacy or effectiveness of VNS.

Conflict of interest

AB received funding from Synergia Medical and the Walloon Region as part of an Industrial Doctorate Program (n°8193). PD is employed by Synergia Medical. AN is a member of the Scientific Council and a shareholder at Synergia Medical. The funder was not involved in the study design, data collection and analysis, interpretation of the data, the writing of the article, or the decision to submit it for publication.

Acknowledgements

This work was supported by the Walloon Region and Synergia Medical SA (Industrial Doctorate Program, convention n°8193). RET is funded by the Walloon Excellence in Life Sciences and

Biotechnology (WELBIO) department of the WEL Research Institute (X.2001.22) and the Queen Elisabeth Medical Foundation (QEMF).

Author contribution

EC and SV were involved in data collection. AB and SV were involved in data analysis. AB was involved in drafting the original manuscript. All authors were involved in the interpretation of the data and the review of the manuscript.

Appendix A. Supplementary data

Supplementary data to this article can be found online at https://doi.org/10.1016/j.clinph.2023.01.009.

References

Ardesch JJ, Sikken JR, Veltink PH, van der Aa HE, Hageman G, Buschman HPJ. Vagus nerve stimulation for epilepsy activates the vocal folds maximally at therapeutic levels. Epilepsy Res 2010;89(2–3):227–31.
Bouckaert C, Raedt R, Larsen LE, El Tahry R, Gadeyne S, Carrette E, Proesman S, et al. Laryngeal Muscle-Evoked Potential Recording as an Indicator of Vagal Nerve Fiber Activation. Neuromodulation 2022:1–10.
Boyd A, Kalu KU. Scaling factor relating conduction velocity and diameter for myelinated afferent nerve fibres in the cat hind limb. Physiol J 1979;289 (1):277–97.
DeGiorgio C, Heck C, Bunch S, Britton J, Green P, Lancman M, Murphy J, et al. Vagus nerve stimulation for epilepsy: randomized comparison of three stimulation paradigms. Neurology 2005:317–9.
Devanne H, Lavoie BA, Capaday C. Input-output properties and gain changes in the human corticospinal pathway. Exp Brain Res 1997:329–38.
El Tahry R, Mollet L, Raedt R, Delbeke J, De Herdt V, Wyckhuys T, Hemelsoet D, et al. Repeated assessment of larynx compound muscle action potentials using a self-sizing cuff electrode around the vagus nerve in experimental rats. J Neurosci Methods 2011;198(2):287–93.
Evans MS, Verma-Ahuja S, Naritoku DK, Espinosa JA. Intraoperative human vagus nerve compound action potentials. Acta Neurol Scand 2004;110(4):232–8.
Fahoum F, Boffini M, Kann L, Faini S, Gordon C, Tzadok M, El Tahry R. VNS parameters for clinical response in Epilepsy. Brain Stimul 2022;15(3):814–21.
Fiest KM, Sauro KM, Wiebe S, Patten SB, Kwon CS, Dykeman J, Pringsheim T, Lorenzetti DL, Jetté N. Prevalence and incidence of epilepsy: A systematic review and meta-analysis of international studies. Neurology 2017;88 (3):296–303.
Grimonprez A, Raedt R, De Taeye L, Larsen LE, Delbeke J, Boon P, Vonck K. A Preclinical Study of Laryngeal Motor-Evoked Potentials as a Marker Vagus Nerve Activation. Int J Neural Syst 2015;1550034:1–10.
Heck C, Helmers SL, DeGiorgio CM. Vagus nerve stimulation therapy, epilepsy, and device parameters: scientific basis and recommendations for use. Neurology 2002:31–7.
Hill PD. Kernel estimation of a distribution function. Commun Stat 1985;14 (3):605–20.
Kamani D, Potenza AS, Cernea CR, Kamani YV, Randolph GW. The nonrecurrent laryngeal nerve: anatomic and electrophysiologic algorithm for reliable identification. Laryngoscope 2015;125(2):503–8.
Kawai K, Tanaka T, Baba H, Bunker M, Ikeda A, Inoue Y, Kameyama S, et al. Outcome of vagus nerve stimulation for drug-resistant epilepsy: the first three years of a prospective Japanese registry. Epileptic Disord 2017;19(3):327–38.
Kayyali H, Abdelmoity S, Bansal L, Kaufman C, Smith K, Fecske E, Pawar K, et al. The Efficacy and Safety of Rapid Cycling Vagus Nerve Stimulation in Children With Intractable Epilepsy. Pediatr Neurol 2020:35–8.
Krahl SE. Vagus nerve stimulation for epilepsy: A review of the peripheral mechanisms. Surg Neurol Int 2012;3:47–52.
Krahl SE, Clark KB, Smoth DC, Browning RA. Locus coeruleus lesions suppress the seizure-attenuating effects of vagus nerve stimulation. Epilepsia 1998;39 (7):709–14.
Kwan P, Arzimanoglou A, Berg AT, Brodie MJ, Hauser WA, Mathern G, Moshé SL, Perucca E, Wiebe S, French J. Definition of drug resistant epilepsy: consensus proposal by the ad hoc Task Force of the ILAE Commission on Therapeutic Strategies. Epilepsia 2010;51(6):1069–77.
Loerwald KW, Borland MS, Rennaker RL, Hays SA, Kilgard MP. The interaction of pulse width and current intensity on the extent of cortical plasticity evoked by vagus nerve stimulation. Brain Stimul 2018;11(2):271–7.
Morrison RA, Hulsey DR, Adcock KS, Rennaker RL, Kilgard MP, Hays SA. Vagus Nerve Stimulation Intensity Influences Motor Cortex Plasticity. Brain Stimul 2020a;12 (2):256–62.
Morrison RA, Danaphongse TT, Pruitt DT, Adcock KS, Mathew JK, Abe ST, Abdulla DM, Rennaker RL, Kilgard MP, Hays SA. A limited range of vagus nerve stimulation intensities produce motor cortex reorganization when delivered during training. Behav Brain Res 2020b;391 112705.
Morrison RA, Danaphongse TT, Abe ST, Stevens ME, Ezhil V, Seyedahmadi A, Adcock KS, Rennaker RL, Kilgard MP, Hays SA. High intensity VNS disrupts VNS-mediated plasticity in motor cortex. Brain Res J 2021;1756 147332.
Pedregosa F, Varoquaux G, Gramfort A, Michel V, Thirion B, Grisel O, Blondel M, et al. Scikit-learn: Machine Learning in Python. J Mach Learn Res 2011;12:2825–30.
Pruitt DT, Danaphongse TT, Patel M, Luchtman N, Reddy P, Wang V, et al. Optimizing Dosing of Vagus Nerve Stimulation for Stroke Recovery. Transl Stroke Res 2021;12:65–71.
Raedt R, Clinckers R, Mollet L, Vonck K, El Tahry R, Wyckhuys T, De Herdt V, et al. Increased hippocampal noradrenaline is a biomarker for efficacy of vagus nerve stimulation in a limbic seizure model. J Neurochem 2011;117(3):461–9.
Rijkers K, Aalbers M, Hoogland G, van Winder L, Vles J, Steinbusch H, Majoie M. Acute seizure-suppressing effect of vagus nerve stimulation in the amygdala kindled rat. Brain Res J 2010;1319:155–63.
Souza RR, Robertson NM, McIntyre CK, Rennaker RL, Hays SA, Kilgard MP. Vagus nerve stimulation enhances fear extinction as an inverted-U function of stimulation intensity. Exp Neurol 2021;341 113718.
Toffa DH, Touma L, El Meskine T, Bouthillier A, Nguyen DK. Learnings from 30 years of reported efficacy and safety of vagus nerve stimulation (VNS) for epilepsy treatment: A critical review. Seizure 2020;83:104–23.
Vespa S, Stumpp L, Bouckaert C, Delbeke J, Smets H, Cury J, Ferrao Santos S, et al. Vagus Nerve Stimulation-Induced Laryngeal Motor Evoked Potentials: A Possible Biomarker of Effective Nerve Activation. Front Neurosci 2019;13:880.
Woodbury DM, Woodbury JW. Effects of vagal stimulation on experimentally induced seizures in rats. Epilepsia 1990;31:7–19.
Yamamoto T. Vagus Nerve Stimulation Therapy: Indications, Programming and Outcomes. Neurol Med Chir 2015:407–15.